EPJ Web of Conferences **119**, 08001 (2016) DOI: 10.1051/epjconf/201611908001
ILRC 27

VERTICAL VARIATION OF OPTICAL PROPERTIES OF MIXED ASIAN DUST/POLLUTION PLUMES ACCORDING TO PATHWAY OF AIRMASS TRANSPORT OVER EAST ASIA

Sung-Kyun Shin [1]*, Detlef Müller[2], K.H. Lee[3], D. Shin[4], Y. J. Kim[1], Y. M. Noh[5]

[1]*Gwangju Institute of Science and Technology (GIST), Republic of Korea, *Email: skyun@gist.ac.kr*

[2]*Uiversity of Hertfordshire, United Kingdom*

[3]*Ganneung-Wonju National University, Republic of Korea*

[4]*National Institute of Environmental Research, Republic of Korea*

[5]*Ineternational Environmental Research Center (IERC), GIST, Republic of Korea*

ABSTRACT

We use five years (2009 – 2013) of multiwavelength Raman lidar measurements at Gwangju, Korea (35.10° N, 126.53° E) for the identification of changes of optical properties of East Asian dust in dependence of its transport path over China. Profiles of backscatter and extinction coefficients, lidar ratios, and backscatter-related Ångström exponents (wavelength pair 355/532nm) were measured at Gwangju. Linear particle depolarization ratios were used to identify East Asian dust layers. We used backward trajectory modelling to identify the pathway and the vertical position of dust-laden air masses over China during long-range transport. Most cases of Asian dust events can be described by the emission of dust in desert areas and subsequent transport over highly polluted regions of China. The Asian dust plumes could be categorized into two classes according to the height above ground in which these plumes were transported: (I) the dust layers passed over China at high altitude levels until arrival over Gwangju, and (II) the Asian dust layers were transported near the surface and the lower troposphere over industrialized areas before they arrived over Gwangju. We find that the optical characteristics of these mixed Asian dust layers over Gwangju differ in dependence of their vertical position above ground over China and the change of height above ground during transport. The mean linear particle depolarization ratio was 0.21±0.06 (at 532 nm), the mean lidar ratios were 52±7 sr at 355 nm and 53±8 sr at 532 nm, and the mean Ångström exponent was 0.74±0.31 in case I. In contrast, plumes transported at lower altitudes (case II) showed low depolarization ratios, and higher lidar ratio and Ångström exponents. The mean linear particle depolarization ratio was 0.13 ± 0.04, the mean lidar ratios were 63±9 sr at 355 nm and 62±8 sr at 532 nm, respectively, and the mean Ångström exponent was 0.98±0.51. These numbers show that the optical characteristics of mixed Asian plumes are more similar to optical characteristics of urban pollution.

1. INTRODUCTION

East Asian dust is particularly complicated as it usually travels over densely populated and highly industrialized areas of China before it moves out over Pacific Ocean. During transport over East Asia dust mixes with pollutants such as industrial soot, toxic material, and acidic gases (Sun et al., 2005). However, there exist few studies on the degree of mixing that occurs between dust and pollution during transport, the effect of the direction of dust transport across China, and the vertical distribution of Asian dust layers during long-range transport over China. There still is a lack of understanding of how much of the mixing of dust with pollutants depends on the vertical distribution over East Asia when dust passes over source regions of anthropogenic pollution. One reason of our limited knowledge is that there are only few vertically-resolved, long-term observations of pollution over East Asia. In this study we use Raman lidar data taken at Gwangju, South Korea, between 2009 and 2013. In our study we focus specifically on lidar observations of Asian dust layers as they passed over China. The main objective of this study is to investigate the variation of optical properties of mixtures of Asian dust with anthropogenic pollution in dependence of the pathways and vertical distributions of these mixed dust layers during long-range transport. We identify these dust layers by the linear particle depolarization ratio. We present vertically-resolved optical properties such as lidar ratio and Ångström exponent. We also categorize the optical properties of these pollution plumes according to their transport pathway and their vertical distribution. Section 2 presents the methods used in this study. Section 3 presents our results. We discuss our results and summarize our findings in section 4.

2. METHODOLOGY

The lidar station, dubbed MRS.LEA (Multi-wavelength Raman Spectrometer Lidar in East Asia) of the Gwangju Institute of Science and Technology (GIST) is located at 35.10° N, 126.53° E in the west-south-western part of the Korean peninsula. A description of the lidar system is given by Noh et al. (2008). The system allows us to retrieve vertical profiles of the particle backscatter coefficients at 355, 532, and 1064 nm, the particle extinction coefficients at 355 and 532 nm, the linear particle depolarization ratio at 532 nm, the water-vapor mixing-ratio, and profiles of silicon-dioxide (Müller et al., 2010). Profiles of silicon-dioxide (quartz) can be used as tracer of the concentration of mineral dust. In this contribution we use the signals needed for measuring particle backscatter and extinction coefficients at 355 and 532 nm and the linear particle depolarization ratio. The profiles of particle backscatter coefficients ($\boldsymbol{\beta}_{\mathbf{p}}$) at 355 and 532 nm were calculated with the Raman method. The overlap effect which describes the incomplete overlap between outgoing laser beam and field of view of the receiver telescope is cancelled out for the case of profiles of the backscatter coefficient because the ratios of two signals (elastic signals from particles and molecules and the nitrogen Raman signals) are. In that way we can retrieve vertical profiles of the backscatter coefficient to 400 m above ground. The vertical profiles of the aerosol extinction coefficients ($\boldsymbol{\alpha}_{\mathbf{p}}$) at 355 and 532 nm were derived with the use of the nitrogen vibration Raman signals at 387 and 607 nm, respectively. We derive particle extinction-to-backscatter ratios (lidar ratios, denoted as $\boldsymbol{S}$ in this contribution) at 355 and 532 nm from the profiles of $\boldsymbol{\beta}_{\mathbf{p}}$ and $\boldsymbol{\alpha}_{\mathbf{p}}$. The backscatter-related Ångström exponent for the wavelength pair of 355/532 nm (denoted as $\boldsymbol{\mathring{A}}_{\boldsymbol{\beta}}$) is computed, too. The measurements were carried out at nighttime under cloud-free conditions. In this contribution we use the linear particle depolarization ratio according to the definition by as below:

$$\delta_{\mathrm{p}} = \frac{\delta(z)\mathrm{R_B}(z) - \delta_{\mathrm{m}}}{\mathrm{R_B}(z) - 1}.$$

The term $\boldsymbol{\delta}_{\mathbf{m}}$ is the linear depolarization ratio of air molecules at the wavelength and bandwidth of the emitted laser wavelength. We used the value $\boldsymbol{\delta}_{\mathbf{m}}$=0.0044 (Behrendt and Nakamura, 2002). This value takes account of our interference filter which have a full width at half maximum of 1.0 nm. $\boldsymbol{R}_{\mathbf{B}}(\mathbf{z})$ is the backscatter ratio, expressed as $(\boldsymbol{\beta}_{\mathbf{p}}+\boldsymbol{\beta}_{\mathbf{m}})/\boldsymbol{\beta}_{\mathbf{m}}$ at altitude *z*. $\boldsymbol{\beta}_{\mathbf{m}}$ denotes the backscatter coefficient of atmospheric molecules. The calibration of the polarization channels was carried out by using rotating polarizers following the methodology explained by Tesche et al. (2009).

3. RESULTS

Figure 1 shows the transport pathway and the change of the vertical position of the dust plumes during transport to our lidar site. It is clear that backward trajectories cannot provide us with information on the concentration of dust and anthropogenic pollution in the air masses prior to observation over Korea. Still, backward trajectories show if the air masses originated from or nearby the desert regions, and whether the air masses passed over densely populated/industrialized regions. Case I includes those Asian dust plumes that passed over industrialized areas in China at high altitude level (> 3km height above ground) as shown in figure 6a. The Asian dust plumes were classified as Case II when they were transported through the near surface/lower troposphere (< 3km height above ground) over industrialized areas in China, i.e., longitude range between 110° E and 125° E; the locations of industrialized and densely populated regions in China are shown in figure 1. The depolarization ratios of the Asian dust plumes we observed are lower compared to depolarization ratios of pure dust particles. For example, Freudenthaler et al. (2009) report a value of $\boldsymbol{\delta_p}$ = 0.31 at 532 nm for pure Saharan dust observed during SAMUM 2006. The values of $\boldsymbol{\delta_p}$ and the corresponding values of $\boldsymbol{\mathring{A}_\beta}$ and $\boldsymbol{S}$ at 355 nm and 532 nm for the Cases I and II are also shown in figure 1.

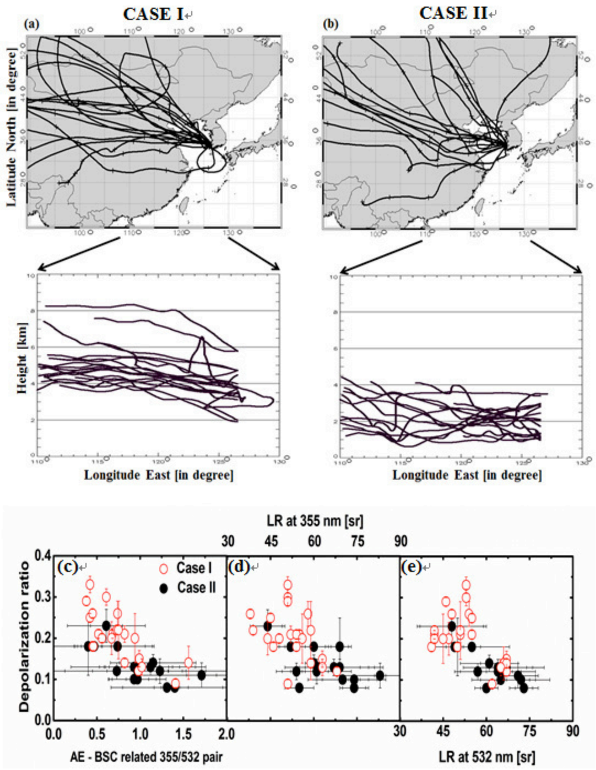

Figure 1. (top panel) Transport pattern of the dust plumes that originated in the desert regions and passed over industrialized/populated regions of China before arrival over the Korean peninsula. (middle panel) Vertical position of the dust layers during transport: (a) Dust layers passed over China at high altitude (Case I) (b) dust layers were transported over China through the near surface/lower troposphere (Case II). (bottom panel) Scatter diagram of the linear particle depolarization at 532 nm versus (c) the backscatter-related Ångström exponent (355/532 nm wavelength pair), and the (d), (e) lidar ratio (at 355 nm and at 532 nm) with respect to the Case I and Case II. The two categories I, II are denoted by different colors.

We find different clusters of the optical properties of the dust layers when we take into consideration their vertical position during transport. Cases I show larger values of $\boldsymbol{\delta_p}$ compared to case II. On average $\boldsymbol{\mathring{A}_\beta}$ of case I is smaller than $\boldsymbol{\mathring{A}_\beta}$ of case II. The average values of $\boldsymbol{\delta_p}$ and $\boldsymbol{\mathring{A}_\beta}$ are 0.21±0.06 and 0.74±0.31, respectively, for case I. In contrast, $\boldsymbol{\delta_p}$ and $\boldsymbol{\mathring{A}_\beta}$ are 0.13±0.04 and 0.98±0.35, respectively, for case II. The lowest values of $\boldsymbol{S}$ at 355 nm and 532 nm are also measured for high values of $\boldsymbol{\delta_p}$ (0.21±0.06). We find values of 52±7 sr at 355 nm and 53±8 sr at 532 nm, respectively, for case I. Comparably high values of $\boldsymbol{S}$ were found for case II, i.e. 63±9 at 355 nm and 62±8sr at 532 nm. In that case the value of $\boldsymbol{\delta_p}$ is 0.13±0.04. There are several previous studies that report on depolarization ratios of polluted dust after long-range transport. According to these studies the observed dust particles were partly/completely mixed with anthropogenic pollution (Shimizu et al., 2004; Chen et al., 2007). As a result of the mixing of dust with anthropogenic pollution, the values of $\boldsymbol{\delta_p}$ were lower than the values of pure dust, which is estimated to be at 0.3 - 0.35 (Murayama et al., 2004; Freudenthaler et al., 2009). Likewise, the values of $\boldsymbol{\mathring{A}_\beta}$ and $\boldsymbol{S}$ also differ compared to the values of $\boldsymbol{\mathring{A}_\beta}$ and $\boldsymbol{S}$ of pure dust. We assume that the dust particles carried more anthropogenic pollution in cases where the air masses travelled near the surface. Consequently, the optical characteristics of the dust/pollution layers of case II are dominated by the optical properties of anthropogenic pollutants. In contrast, the optical properties of dust layers that travelled at high altitudes (Case I) are less influenced by urban/industrial pollutants. Thus, the optical properties of these dust layers are more likely to be those of pure dust. The clusters denoted Case I and Case II were classified according to the altitude the dust-laden air masses passed over industrialized/populated regions of China. The differences of the optical properties of the dust layers are shown in figure 2. The difference of the optical characteristics of East Asian dust layers that travelled in surface-near heights and at high altitudes is obvious. The values of $\boldsymbol{\delta_p}$, $\boldsymbol{\mathring{A}_\beta}$ and $\boldsymbol{S}$ are 0.12±0.01, 1.00±0.43, and 63±7 sr at 355 nm and 64±6 sr at 532 nm, respectively, when Asian dust passed over China below 1 km height above ground. These values reflect the fact that the optical properties of the dust/pollution plumes are dominated by the anthropogenic part of the particles in these plumes. In contrast, the values of $\boldsymbol{\delta_p}$, $\boldsymbol{\mathring{A}_\beta}$, and $\boldsymbol{S}$ were 0.23±0.02, 0.60±027, and 50±7 sr at 355 nm and 49±8 sr at 532 nm, respectively, when the dust layers passed over China at high altitudes, i.e., above 4 km. These values more likely reflect the optical characteristic of Asian dust particles that are less affected by the contribution of anthropogenic pollution. The altitude in which the Asian dust layers passed over China have significant influence on their optical characteristics. In our study, we took 3 km above ground as threshold value as we observed a notable change of optical properties of the dust/pollution plumes if they travelled below or below 3 km height above ground. Pollution particles below 3 km could mix and interact with Asian dust particles (more influence). In contrast, we assume that optical properties of dust particles above 3 km are not that much influenced by anthropogenic pollution as the mixing of pollution into these heights is less intense. This height of 3 km is also in relatively good agreement with the average height of planetary boundary layers. Pollutants emitted at the surface predominantly stay in this height (Basha et al., 2009).

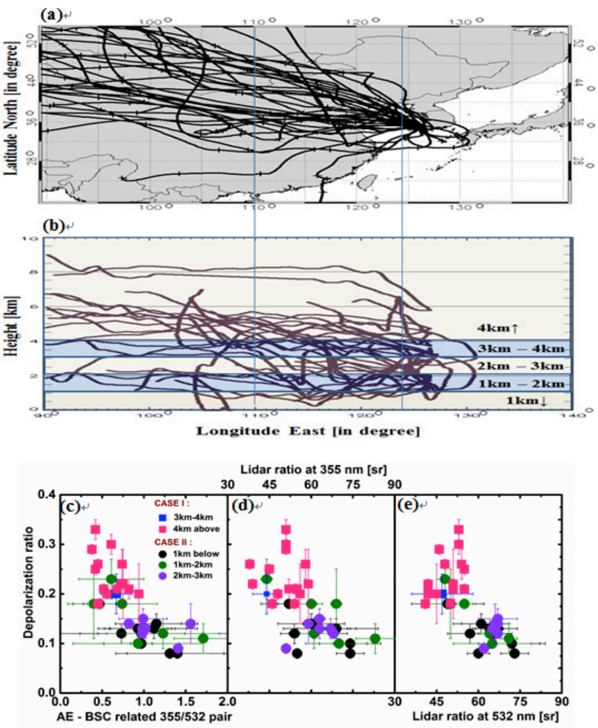

Figure 2. (top panel) (a) the transport pathway and the classification of East Asian dust layers with respect to (b) their altitude above ground when they passed over industrial regions of China. (bottom panel) Scatter plots of the linear particle depolarization at 532 nm versus (c) the backscatter-related Ångström exponent (355/532 nm wavelength pair), versus (d) the lidar ratio at 355 nm, respectively (e) the lidar ratio at 532 nm in dependence of the 5 altitude categories. The height of the Asian dust layers above ground is denoted by different colors and symbols. Case I included the layers from 3 – 4 km and above 4 km (blue and pink colored squares). Case II includes the layers from 0 - 1 km, from 1-2km, and from 2-3km height above ground (black, green and violet circles).

4. CONCLUSIONS

Our results suggest that the transport pathway as well as the vertical position of Asian dust during long-range transport may have significant impact on the optical properties of mixed Asian dust layers.

ACKNOWLEDGEMENT

This work was supported by the "Advanced Research on Applied Meteorology" of National Institute of Meteorological Research (NIMR) funded by the Korea Meteorological Administration (KMA) and the Eco-Innovation Project 2012000160004 from Korean Ministry of Environment through the Advanced Environmental Monitoring Research Center.

REFERENCES

[1] Basha, G., and Ratnam, M. V., 2009: Identification of atmospheric boundary layer height over a tropical station using high-resolution radiosonde refractivity profiles: Comparison with GPS radio occultation measurements, Journal of Geophysical Research: Atmospheres (1984–2012), **114**.

[2] Behrendt, A., and Nakamura, T., 2002: Calculation of the calibration constant of polarization lidar and its dependency on atmospheric temperature, Optics express, **10**, 805-817

[3] Chen, W.-N., Chen, Y.-W., Chou, C. C., Chang, S.-Y., Lin, P.-H., and Chen, J.-P., 2009: Columnar optical properties of tropospheric aerosol by combined lidar and sunphotometer measurements at Taipei, Taiwan, Atmospheric Environment, **43**, 2700-2708.

[4] Freudenthaler, V., Esselborn, M., Wiegner, M., Heese, B., Tesche, M., Ansmann, A., Müller, D., Althausen, D., Wirth, M., and Fix, A., 2009: Depolarization ratio profiling at several

wavelengths in pure Saharan dust during SAMUM 2006, Tellus B, **61**, 165-179.

[5] Müller, D., Mattis, I., Tatarov, B., Noh, Y., Shin, D., Shin, S., Lee, K., Kim, Y., and Sugimoto, N., 2010: Mineral quartz concentration measurements of mixed mineral dust/urban haze pollution plumes over Korea with multiwavelength aerosol Raman-quartz lidar, Geophysical Research Letters, **37**.

[6] Murayama, T., Müller, D., Wada, K., Shimizu, A., Sekiguchi, M., and Tsukamoto, T., 2004: Characterization of Asian dust and Siberian smoke with multi-wavelength Raman lidar over Tokyo, Japan in spring 2003, Geophysical Research Letters, **31**.

[7] Noh, Y. M., Kim, Y. J., and Müller, D., 2008: Seasonal characteristics of lidar ratios measured with a Raman lidar at Gwangju, Korea in spring and autumn, Atmospheric Environment, **42**, 2208-2224.

[8] Shimizu, A., Sugimoto, N., Matsui, I., Arao, K., Uno, I., Murayama, T., Kagawa, N., Aoki, K., Uchiyama, A., and Yamazaki, A., 2004: Continuous observations of Asian dust and other aerosols by polarization lidars in China and Japan during ACE-Asia, Journal of Geophysical Research: Atmospheres (1984–2012), **109**.

[9] Sun, Y., Zhuang, G., Wang, Y., Zhao, X., Li, J., Wang, Z., and An, Z., 2005: Chemical composition of dust storms in Beijing and implications for the mixing of mineral aerosol with pollution aerosol on the pathway, Journal of Geophysical Research: Atmospheres (1984–2012), **110**.

[10] Tesche, M., Ansmann, A., Müller, D., Althausen, D., Mattis, I., Heese, B., Freudenthaler, V., Wiegner, M., Esselborn, M., and Pisani, G., 2009: Vertical profiling of Saharan dust with Raman lidars and airborne HSRL in southern Morocco during SAMUM, Tellus B, **61**, 144-164.